Tuijin Jishu/Journal of Propulsion Technology
ISSN: 1001-4055
Vol. 44 No. 3 (2023)

Performance of Switched Inductor-qZSI on different Controls Methods for PV Application

[1] Chandra Shekhar Singh Chandal, [2] Saket Kumar Singh, [3] Ajit Kumar

[1] Assistant Professor, Department of Electrical & Electronics Engineering
Motihari College of Engineering, (Under the Department of Science, Technology and Technical Education, Government of Bihar), Motihari, Bihar, India
[2] Assistant Professor, Department of Electrical & Electronics Engineering
Motihari College of Engineering, (Under the Department of Science, Technology and Technical Education, Government of Bihar), Motihari, Bihar, India
[3] Assistant Professor, Department of Electrical & Electronics Engineering
Gaya college of Engineering, (Under the Department of Science, Technology and Technical Education, Government of Bihar), Gaya, Bihar, India

Abstract: The performance of the Switched Inductor Quasi Impedance Source Inverter (SL-qZSI) for the Simple, Maximum, and Maximum Constant Boost Control Methods for PV Application is compared in this study. Because a second DC-DC converter must be added to the inverter circuit to achieve the desired output due to the significant voltage differential between the AC output side and the DC input side, the suggested control technique intends to increase the efficiency of the DC/AC converter. This two-stage system i.e., DC-DC conversion and then DC to AC conversion not only reduces the efficiency but also dilutes the dynamic response. Researchers have recently suggested alternative ZSI to maximize the boost factor and enhance the functionality of the inverters (Input Side). To satisfy both requirements, SL-qZSI is suggested. The SL-qZSI enhances input current and reliability compared to conventional ZSI. Additionally, compared to other ZSI, the proposed SL-qZSI has lower shoot-through (ST) current, current stress on inductors & diodes, and voltage stress on capacitors. Additionally, it prevents the starting inrush current, which may harm the equipment. The boost factor and gain of the maximum boost control are found to be high compared to others for the same value of the modulation index in the control component, but a large inductor is needed due to the significant ripple in the input current and shoot-through current. The inductor's high value results in an increase in both the inverter's size and price. Results from simulations have been run under the PV panel's Standard Test settings.
Keywords Impedance network, impedance source inverter, Constant-boost, shoot-through, Maximum-boost, PWM, Renewable energy, DC-DC converters, Photovoltaic (PV), Electric Vehicle, Efficiency, QZSI, SL-qZSI and Stability

1. Introduction

In the present scenario we all are aware that there is an increase in the demand for Converters and their control algorithms in the field of Electric vehicle charging, EV drives and photovoltaic (PV) solar energy system, integration of micro-grids, and wireless energy transfer[1]–[5]. It is imperative to create renewable, highly efficient, and clean forms of energy due to the depletion of fossil fuels, rising environmental concerns, and increasing electrical energy consumption worldwide. The development of several alternatives includes Solar PV, one of the most promising renewable energy sources. Unfortunately, the PV arrays are low-voltage dc sources, necessitating a large step-up dc-dc converter to convert to a higher voltage. Before attaching it to a dc-ac inverter for grid- related applications, as seen in Fig. 1[6]. The solar photovoltaic system can be utilized in grid-interactive mode, which supplies power to a utility grid, or in stand-alone mode, which supplies power directly to the load. Whenever a solar PV system feeds ac loads in stand-alone mode or feeds the utility grid at a specific voltage and frequency, it always needs an interface inverter[7]. Renewable energy sources or batteries provide DC input voltage and Converting DC input sources to AC output waveforms is essential in most applications. Conventionally, there are two kinds of inverters, VSI (Voltage Source Inverters) and CSI (Current Source Inverters) which are used for energy conversion between DC voltage sources and AC load. Also, when there is an enormous variation between AC output voltage and DC input voltage, another DC-DC converter is added at the input side of the inverter to adjust the output voltage level. This two-stage system (DC-DC and then DC-AC) not only decrease the dynamic response but also reduces the system's efficiency[8]. In conventional inverters, the

presence of dead time between the two switches of the same leg is required to avoid short circuit failure. But it will create distortion in the waveform. By using an Impedance-source inverter (ISI) developed by F.Z. Peng, this issue is improved. Because of advances in technology, improved versions of the Z source inverters have been developed by researchers. Quasi Z-source inverters (q-ZSI), Switched Inductor impedance source inverters (SL-ZSI) and Switched Inductor Quasi ZSI are advanced versions of the ZSI family that have a high boost factor as compared to the conventional ZSI[9]–[12]. Controlling the conventional and advanced ZSI is also very important in improving performance. The control of SL-ZSI involves, how and what width of the ST (shoot-through) pulse is inserted in the SPWM (Sine Pulse Width Modulation). So based on ST width, three control methods for PV application are discussed in this paper i.e. SBC (Simple Boost Control), MBC (Maximum Boost Control), and MCB Control (Maximum Constant Boost Control)[13].

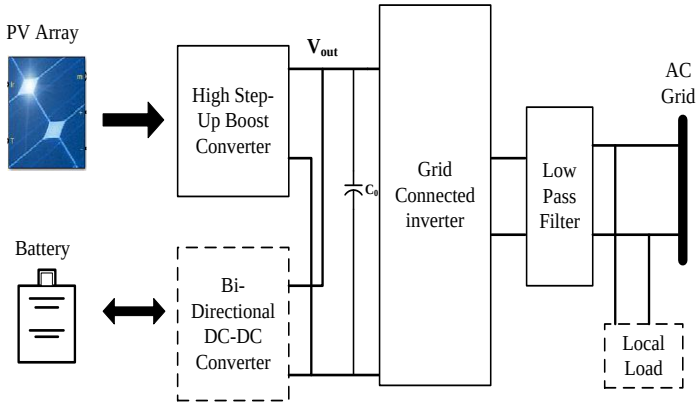

Fig 1: The PV grid-connected system.

2. Switched-Inductor

In this paper, SL-qZSI has been used for continuous input current to examine various control techniques. As compare to the q-ZSI, Three diodes and one inductor are added in SL-qZSI, but by adding it boost factor increases from $1/ (1-2D_0)$ to $(1+D_0)/ (1-2D_0-D_0^2)$ [10], [11]. For the similar input and output voltages, as compared to SL-ZSI it provides continuous input current, reduces the passive component count, a common ground with the dc source, and the boost factor varies from $1+D_0)/ (1-3D_0)$ to $(1+D_0)/ (1-2D_0-D_0^2)$ [9], [11]. It consists of four diodes (D1, D2, D3 and Din), three inductors (L1, L2, and L3) and two capacitors (C1 and C2). The combination of $D_1–D_2–D_3–L_2–L_3$ acts as a switched-inductor cell.

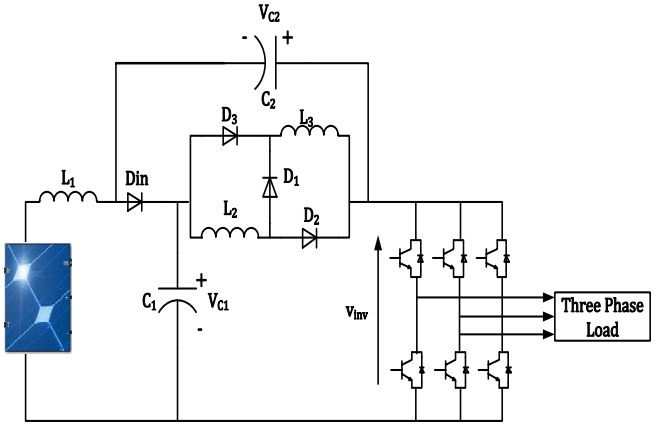

Fig 2: SL-qZSI with continuous input current

2.1 Circuit Analysis of SL-qZSI

Circuit analysis of SL-qZSI is like conventional ZSIs. However, SL-qZSI has an additional ST state other than six active and two zero states. For analysis, the operation of SL-qZSI has been divided into 1. ST State, 2. Non-ST states.

Non-ST state inverter has two zero states and Six active states. During the Non-ST state, D_1 and D_{in} will on, while D_2 and D_3 will be off. Inductor L_2 and L_3 are connected in series. C_1 and C_2 capacitors are charged, while transfer energy takes place from the DC source to the inverter legs through inductors L_1, L_2, and L_3. In this state, voltages across L_2 and L_3 are V_{L2_non} and V_{L3_non}, respectively. We get

$$v_{L1} = v_{C1} - V_0$$
$$v_{L2} = v_{L2_{non}} = v_{C2} - v_{L3_{non}}$$
$$v_{L3} = v_{L3_{non}} = v_{C2} - v_{L2non}$$
$$v_{PN} = v_{C1} + v_{C2}$$

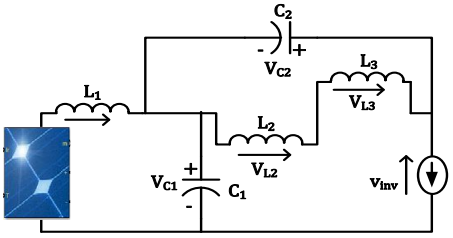

Fig. 2.1.1: Non-shoot-through of SL-qZSI.

In ST (Shoot-Through) State, the switches of the same phase leg are short-circuited. During this state, D_1 and D_{in} are off, while D_2 and D_3 are on, and energy stored in inductor L_1 and inductor L_2 and L_3 are connected in parallel. The energy stored in capacitors C_1 and C_2 gets discharged. In this state voltages across inductors are-

$$v_{L1} = -v_{C2} - V_0$$
$$v_{L2} = v_{L3} = -v_{C1}$$

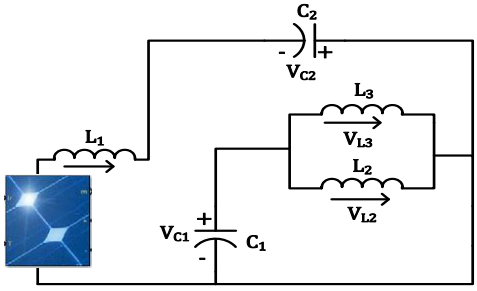

Fig. 2.1.2: Shoot-through of SL-qZSI.

If T_1 and T_0 are the time interval of ST and Non-ST State respectively. then by applying the volt-second balance we obtain: -

$$v_{L2_{non}} = v_{L3_{non}} = \frac{-D_0}{1-D_0} v_{C1} + v_{C2}$$
$$v_{C2} = \frac{2D_0}{1-D_0} v_{C1}$$
$$\begin{cases} v_{C1} = \dfrac{1-D_0}{1-2D_0-D_0^2} V_0 \\ v_{C2} = \dfrac{2D_0}{1-2D_0-D_0^2} V_0 \end{cases}$$

Peak voltage across DC link can be written as-

$$v_{inv} = v_{C1} + v_{C2} = \frac{1+D_0}{1-2D_0-D_0^2} V_0 = B.V_0$$

The boost factor (B) of SL-qZSI is given by-

$$B = \frac{1 + D_0}{1 - 2D_0 - D_0^2} = \frac{1 + \frac{T_0}{T}}{1 - 2\frac{T_0}{T} - (\frac{T_0}{T})^2}$$

For the analysis of the SL-qZSI consider the inductor L_2 and L_3 are same and equal to L current through it. So, the dynamic equations in non-ST state are-

$$L_1 \frac{di_{L1}}{dt} = V_0 + v_{C2}$$
$$L \frac{di_L}{dt} = v_{C1}$$
$$C_1 \frac{dv_{C1}}{dt} = -2i_L$$
$$C_2 \frac{dv_{C2}}{dt} = -i_{L1}$$

For ST state the dynamic equations given by-

$$L_1 \frac{di_{L1}}{dt} = V_0 - v_{C1}$$
$$L \frac{di_L}{dt} = \frac{1}{2} v_{C2}$$
$$C_1 \frac{dv_{C1}}{dt} = i_{L1} - i_{inv}$$
$$C_2 \frac{dv_{C2}}{dt} = i_L - i_{inv}$$

In steady state, for one switching cycle T, So, the average voltage and current across inductor and capacitor respectively are derived as follows: -

$$L_1 \frac{d(i_{L1})_T}{dt} = D_0.(V_0 + v_{C2}) + (1 - D_0).(V_0 - v_{C1}) = 0$$
$$\begin{cases} L \frac{d(i_L)_T}{dt} = D_0.(v_{C1}) + (1 - D_0).(\frac{-1}{2} v_{C2}) = 0 \\ C_1 \frac{d(v_{C1})_T}{dt} = D_0.(-2i_L) + (1 - D_0).(i_{L1} - i_{inv}) = 0 \\ C_2 \frac{d(v_{C2})_T}{dt} = D_0.(-i_{L1}) + (1 - D_0).(i_L - i_{inv}) = 0 \end{cases}$$

The capacitor voltages and inductor currents can be written as:

$$\begin{cases} v_{C1} = \frac{1 - D_0}{1 - 2D_0 - D_0^2} V_0 \\ v_{C2} = \frac{2D_0}{1 - 2D_0 - D_0^2} V_0 \end{cases}$$
$$\begin{cases} i_{L1} = \frac{1 - D_0^2}{1 - 2D_0 - D_0^2} i_{inv} \\ i_{L2} = i_{L3} = i_L = \frac{1 - D_0}{1 - 2D_0 - D_0^2} i_{inv} \end{cases}$$

The input power can be calculated by-

$$P_{input} = I_{input} \cdot V_{input}$$
$$P_{input} = i_{L1} \cdot V_0$$

If losses of the inverter are neglected, then power flowed from the DC side of the inverter is equal to the load power.

During the non-ST state T_1 and the ST state T_0, the DC-link voltage across the inverter bridge is-

$$v_{inv} = \hat{v}_{inv}$$
$$v_{inv} = 0$$

For one switching cycle T the load power can be given by:

$$P_{load} = v_{inv} \cdot i_{inv} = D_0.0 + (1 - D_0).v_{inv} \cdot i_{inv}$$
$$P_{load} = (1 - D_0).v_{inv} \cdot i_{inv}$$

2.2 Parameter Design of SL-qZSI Network

Performance of inverter depends on selecting the parameters of SL-qZSI network elements[14]. The impedance network of the SL-qZSI includes two capacitors and three inductors. The critical values of the capacitances (C_1 & C_2) and the inductances (L_1, L_2 and L_3) of the SL-qZSI are given by: -

$$C_1 = i_{L2}\frac{D_0}{f_s \cdot \Delta v_{C1}}$$
$$C_2 = i_{L2}\frac{D_0}{f_s \cdot \Delta v_{C2}}$$
$$L_1 = (v_{C2} + V_0)\frac{D_0}{2f_s \cdot \Delta i_{L1}}$$

For inductor L_2 and L_3, if L2 = L_3 = L

$$L = v_{C1}\frac{D_0}{f_s \cdot \Delta i_L}$$

3. Control Methods

Boosting factor of the impedance source inverter depends on the shoot-through state because this additional ST state apart from the traditional non-shoot-through state increases DC link voltage which helps to increase boost factor. This work discusses three control strategies based on the width of the shot through. These three control techniques are Maximum Constant Boost (MCB) Control, Maximum Boost (MB) Control, and Simple Boost (SB) Control. Maximum boost control has the widest shoot-through and simple boost control's narrowest, [13]–[19].

S. No	Control Methods	Conversion of Zero State
1	Simple Boost (SB)	Some zero states are converted into ST state.
2	Maximum Boost (MB)	Every zero state is changed into a ST state.
3	Maximum Constant Boost (MCB)	The majority of zero states have been changed into ST States.

For traditional Three Phase Inverter Output Voltage equation is given by:

$$\hat{V}_{out} = \frac{M * B * V_0}{2}$$

The following is the expression of Boost factor for the SL-qZSI:

$$B = \frac{1 + D_0}{1 - 2D_0 - D_0^2}$$

So, from above equation gain for SL-qZSI is given by-

$$G = B.M$$
$$G = M.\frac{(1 + D_0)}{(1 - 2D_0 - D_0^2)}$$

3.1 Simple Boost Control

This control method maintains the six active states in the same manner as in the conventional carrier based PWM by inserting shoot through in all the PWM's traditional zero states throughout one switching cycle. Figure 1 shows the simple boost control method (3.1.1)[22]. the boost factor and voltage gain are given by-

$$Boostfactor(B) = \frac{M-2}{M^2-4M+2}$$

$$VoltageGain(G) = \frac{M.(M-2)}{M^2-4.M+2}$$

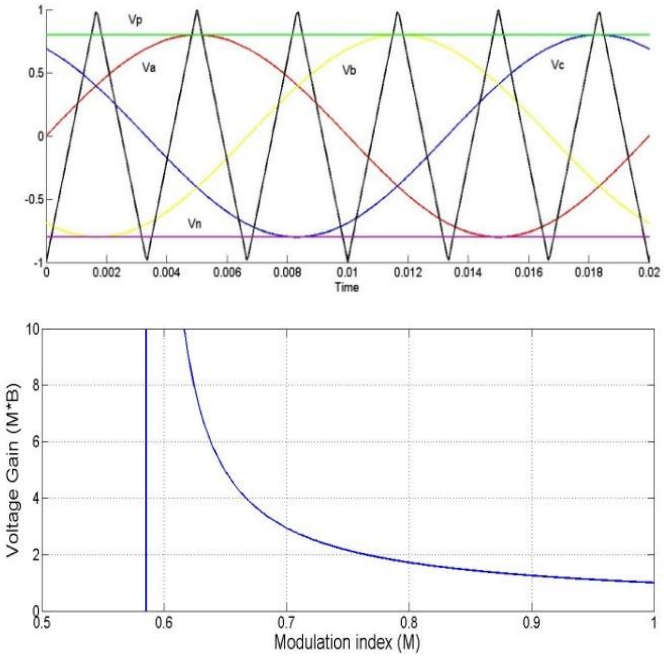

Fig. 3.1.1: Voltage gain of the simple boost control

Voltage stress across the devices is given by

$$V_{inv} = \frac{M-2}{M^2-4M+2} \cdot V_{dc}$$

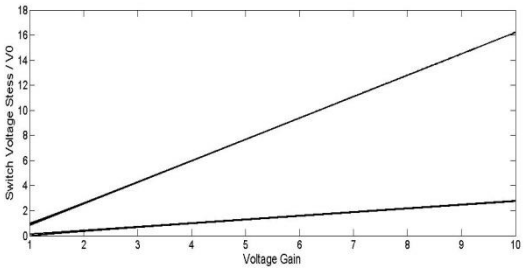

Fig. 3.1.2: Switch voltage stress versus voltage gain for simple boost control

3.2 Maximum Boost Control

The approach for controlling maximum boost is shown in Fig. (3.2.1). The conventional carrier based PWM control approach and this one is quite similar. With this control scheme, all zero states become shoot-through zero states while the six active states remain unaltered. With no distortion to the output waveform, maximum T0 and B are therefore attained for every given modulation index M[15]. the boost factor and voltage gain for MBC are given by-

$$Boostfactor(B) = \frac{8\pi^2-6\sqrt{3}\pi.M}{-8\pi^2+24\sqrt{3}\pi.M-27M^2}$$

$$VoltageGain(G) = \frac{8\pi^2 M - 6\sqrt{3}\pi . M^2}{-8\pi^2 + 24\sqrt{3}\pi . M - 27M^2}$$

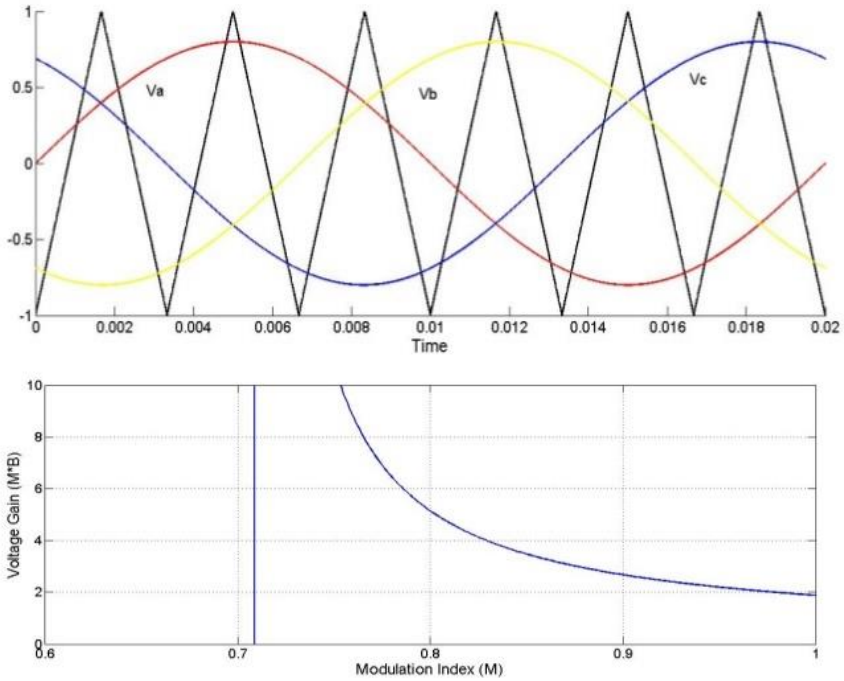

Fig. 3.2.1: Voltage gain of maximum boost control

The devices' voltage stress is determined by-

$$V_{inv} = \frac{8\pi^2 - 6\sqrt{3}\pi . M}{-8\pi^2 + 24\sqrt{3}\pi . M - 27M^2} V_0$$

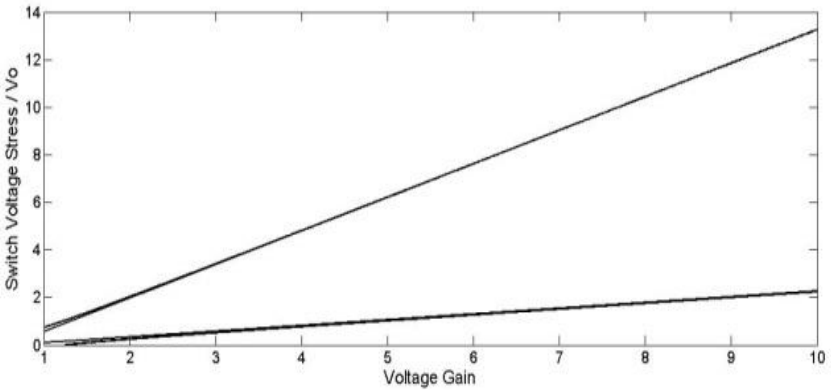

Fig. 3.2.2: Switch voltage stress versus voltage gain for maximum boost control.

3.3 Maximum Constant Boost Control

The shoot-through duty ratio must constantly be consistent in order to reduce volume and cost. To reduce the voltage stress across the switches, a larger voltage boost is desired for any given modulation index. The maximum constant boost control approach is shown in Fig. (3.3.1), which consistently maintains the shoot-through duty ratio while achieving the greatest voltage gain[18]. the boost factor and voltage gain for MCBC are given by-

$$Boostfactor(B) = \frac{8-2\sqrt{3}.M}{-8+8\sqrt{3}.M-3M^2}$$

$$VoltageGain(G) = \frac{8M - 2\sqrt{3}.M^2}{-8 + 8\sqrt{3}.M - 3M^2}$$

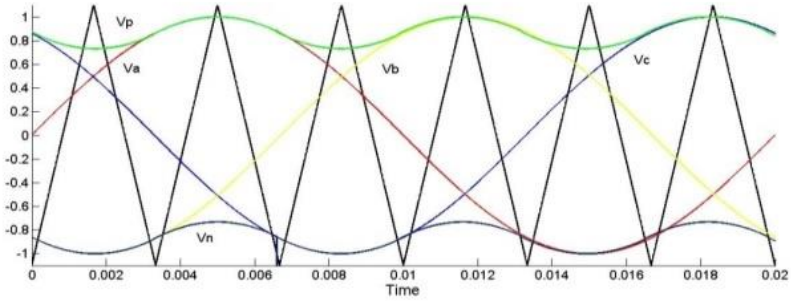

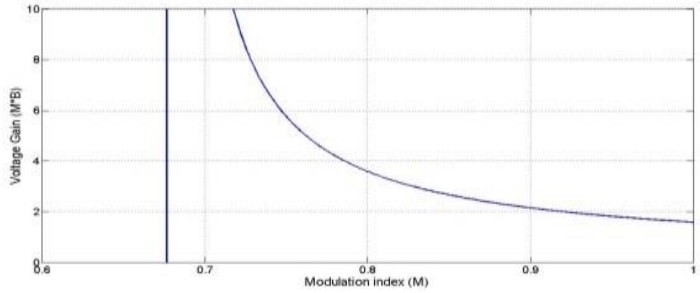

Fig. 3.3.1: Voltage gain of maximum constant boost control

The devices' voltage stress is determined by-

$$V_{inv} = \frac{8 - 2\sqrt{3}.M}{-8 + 8\sqrt{3}.M - 3M^2}V_0$$

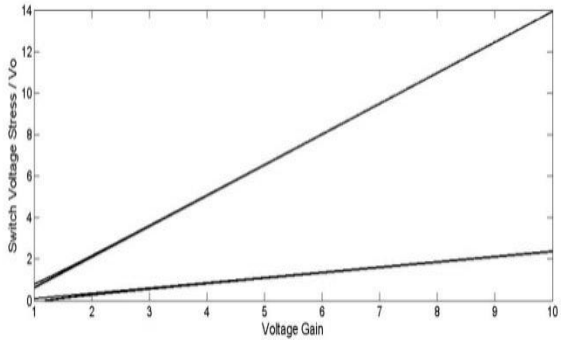

Fig. 3.3.2: Voltage stress versus voltage gain for maximum constant boost control.

3.4 Comparison of Voltage Gain

Expression and plot of Voltage Gain and modulation index of SL-qZSI for different controls are shown below-

Table 1: Comparison of parameters in different control methods

Parameters/ Control methods	SBC	MBC	MCBC
ST Duty ratio (D_0)	$1-M$	$\frac{2\pi-3\sqrt{3}.M}{2\pi}$	$1-\frac{\sqrt{3}M}{2}$
Boost Factor (B)	$\frac{M-2}{M^2-4M+2}$	$\frac{8\pi^2-6\sqrt{3}\pi.M}{-8\pi^2+24\sqrt{3}\pi.M-27M^2}$	$\frac{8-2\sqrt{3}.M}{-8+8\sqrt{3}.M-3M^2}$
Voltage Gain (G)	$\frac{M.(M-2)}{M^2-4.M+2}$	$\frac{8\pi^2M-6\sqrt{3}\pi.M^2}{-8\pi^2+24\sqrt{3}\pi.M-27M^2}$	$\frac{8M-2\sqrt{3}.M^2}{-8+8\sqrt{3}.M-3M^2}$
Voltage Stress across device (Vs)	$\frac{M-2}{M^2-4M+2}V_0$	$\frac{8\pi^2-6\sqrt{3}\pi.M}{-8\pi^2+24\sqrt{3}\pi.M-27M^2}V_0$	$\frac{8-2\sqrt{3}.M}{-8+8\sqrt{3}.M-3M^2}V_0$

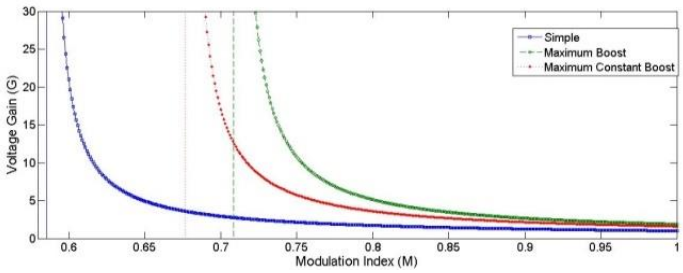

Fig. 3.4: Voltage gain comparison of different control methods

From the plot of Switched Inductor quasi ZSI for different control methods, it is clear that for the same modulation value index gain is maximum in the case of MCB control and minimum for SB.

3.5 Comparison of Voltage Stress

The figure 3.4 shows that the maximum constant boost control approach has somewhat more significant voltage stress than the maximum control method while having significantly lower voltage stress across the devices than the simple control method. Therefore, the voltage-stress ratio should be one. The solution presented in this study is highly desired for applications requiring a voltage gain of two to three. The graphs show that a voltage gain of 2.5 can be attained with just a 30% increase in voltage stress. More importantly, because there are no low-frequency ripples associated with the output voltage in the inductor current and capacitor voltage, this control approach requires the least amount of inductance and capacitance, which lowers the cost, size, and weight of the Impedance-source network. The list of expressions for the various PWM control methods is shown in Table.

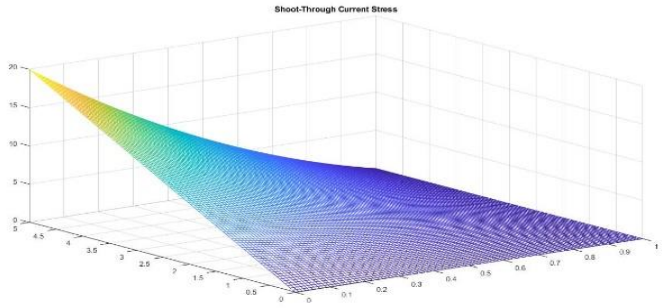

Fig. 3.5.1: Shooth-through Current Stress

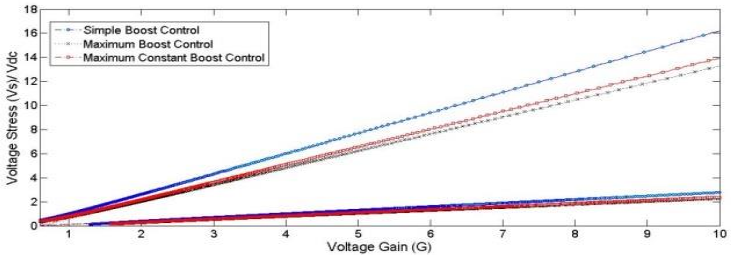

Fig. 3.5.2: Voltage stress comparison of different control methods

Table 2: Component of the proposed converters and those in [6] and [22]– [23].

Refs.	**Components**	**Capacitor Voltage Stress (V_c/V_{dc})**	**Inductor Current Stress (I_L/I_{PN})**	**Input Current**	**Shoot-Through Current Stress (I_{sh}/I_{PN})**	**Boost Factor (B)**	**Gain (G)**	**Average DC-link Current (I_{PN})**
[9]	4 Inductor 2 Capacitor 7 Diode	$\frac{(1-D)B}{1+D}$	$\frac{1-D}{1+D}B$	$0;\ 2I_{L1}-I_{PN}$	$\frac{4(1-D)B}{1+D}$	$\frac{1+D}{1-3D}$	$\frac{4M-\sqrt{3}M^2}{3\sqrt{3}M-4}$	$\frac{(1-D)}{R_l}\hat{V}_{PN}$
[23]	4 Inductor 2 Capacitor 5 Diode	$(1-D)^2B$ $(1-D)B$	$(1-D)B$ $(1-D)^2B$	$0;\ 2I_{L1}-I_{PN}$	$2(1-D)B+2(1-D)^2B$	$\frac{1}{1-4D+2D^2}$	$\frac{2M}{3M^2-2}$	$\frac{(1-D)}{R_l}\hat{V}_{PN}$
[24]	4 Inductor 2 Capacitor 5 Diode	$(1-D)^2B$ $D(1-D)B$ $D(2-D)B$ $\left(1-3D+D^2\right)B$	$\frac{1-D}{1+D}B$ $\frac{2D}{1+D}B$	I_{L1}	$2(1-D)B+2(1-D)^2B$	$\frac{1}{1-4D+2D^2}$	$\frac{2M}{3M^2-2}$	$\frac{(1-D)}{R_l}\hat{V}_{PN}$
Proposed Inverter with MCBC	2 Inductor 2 Capacitor 4 Diode	$(1-D)B$ $(1-D)^2B$	$\frac{1-D}{1+D}B$	I_{L1}	$\frac{(3+D)(1-D)}{1+D}B$	$\frac{1+D}{1-2D-D^2}$	$\frac{8M-2\sqrt{3}.M^2}{-8+8\sqrt{3}.M-3M^2}$	$\frac{(1-D)}{R_l}\hat{V}_{PN}$

4. Simulation Results (Comparisons of Different Control Methods)

The comparison of the various control methods discussed above investigates effectiveness of the different control methods on switched inductor quasi-Impedance-source inverters (SL-qZSI). Simulation of SL-qZSI has performed at the fixed value of modulation index **.8**, input DC voltage 48 V, carrier frequency 10 kHz, Three phase output filters (L_f and C_f) of 20 mH, 30 µF and output load of 1 kilowatt. The value of inductors (L_1=L_2=$L_{3)}$ and capacitors (C_1=$C_{2)}$ used for simulation are 10 mH and 1000 µF. In simulation result this paper compares (as shown in the figure 4.2- 4.10) Shoot-through states, Input current, Voltage across capacitor C_1 & C_2, Voltage across the inverter input, load current and Shoot-through Current (I_{sh}) in different control methods for the same value of modulation index. The block diagram of closed-loop control of SL-qZSI is shown in the figure.

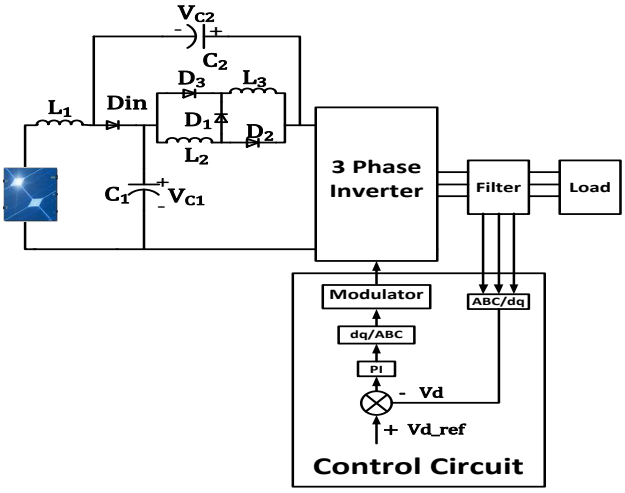

Fig. 4.1: Block diagram of SL-qZSI

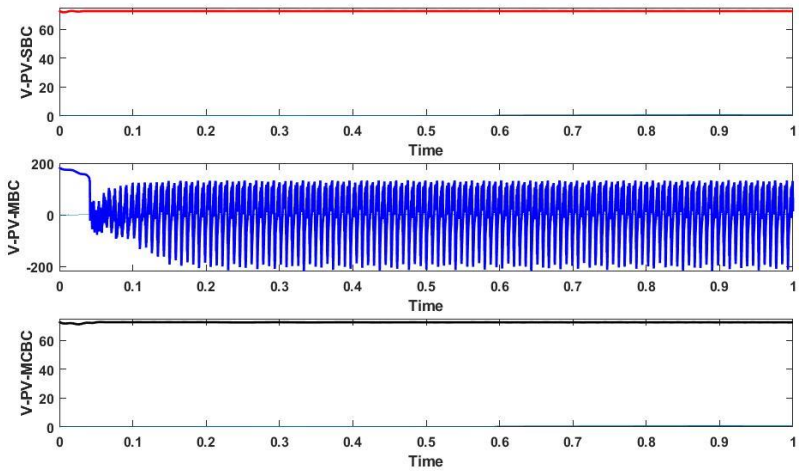

Fig. 4.2: PV-Voltage for different control methods.

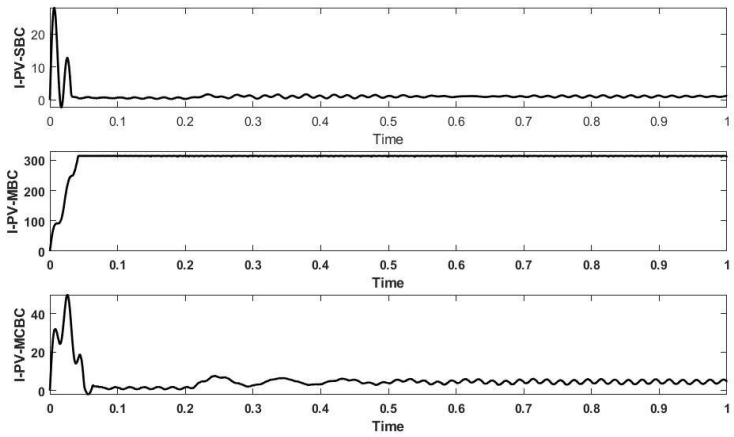

Fig. 4.3: PV- current in different control methods.

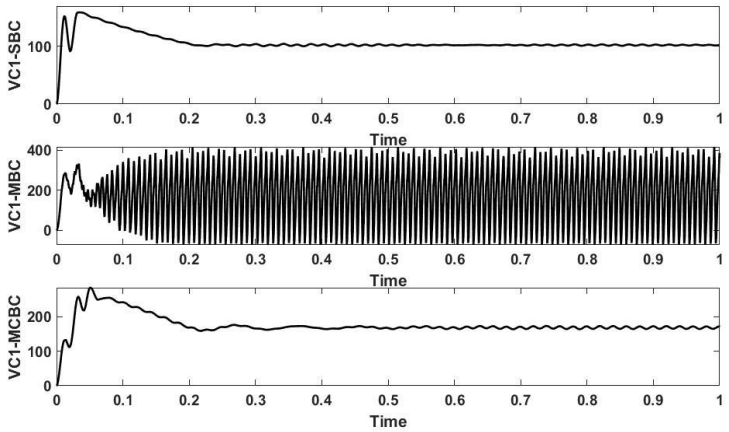

Fig. 4.4: Voltage across capacitor C_1 in different control methods.

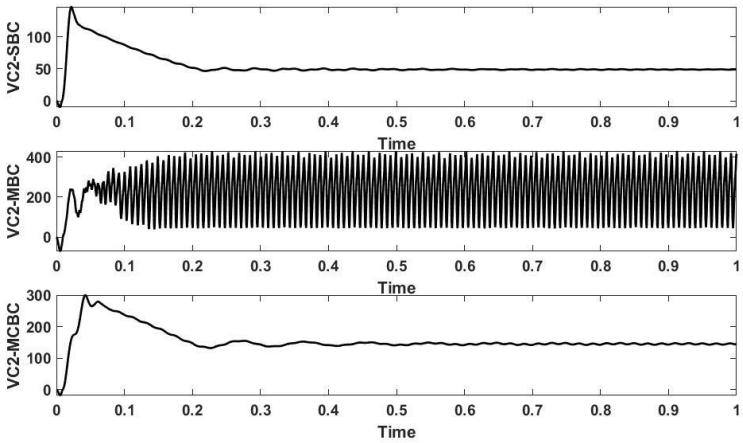

Fig. 4.5: Voltage across capacitor C_2 in different control methods.

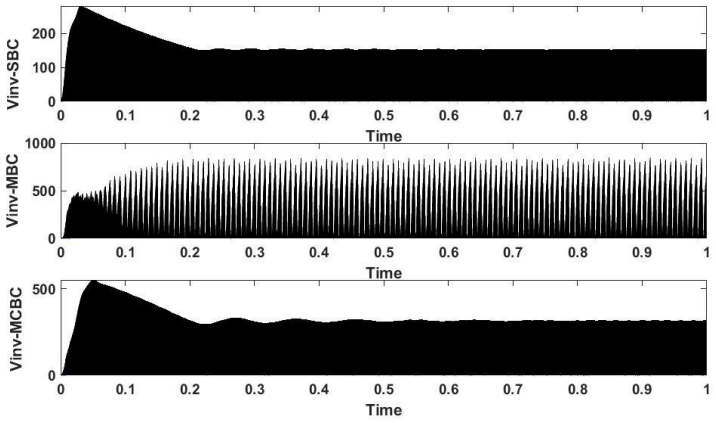

Fig. 4.6: Voltage across the inverter input in different control methods.

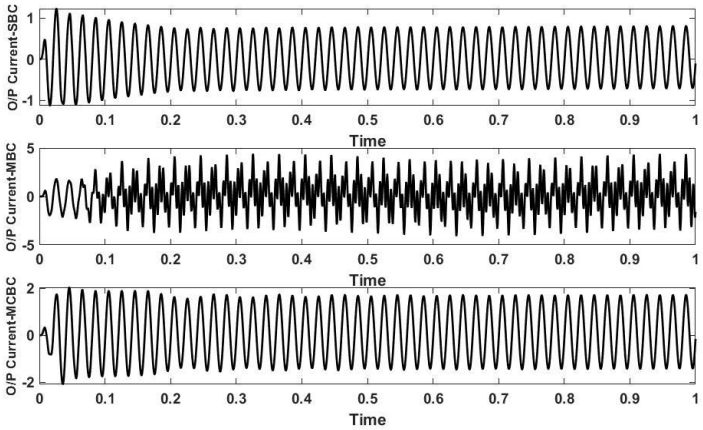

Fig. 4.7: load current in different control methods.

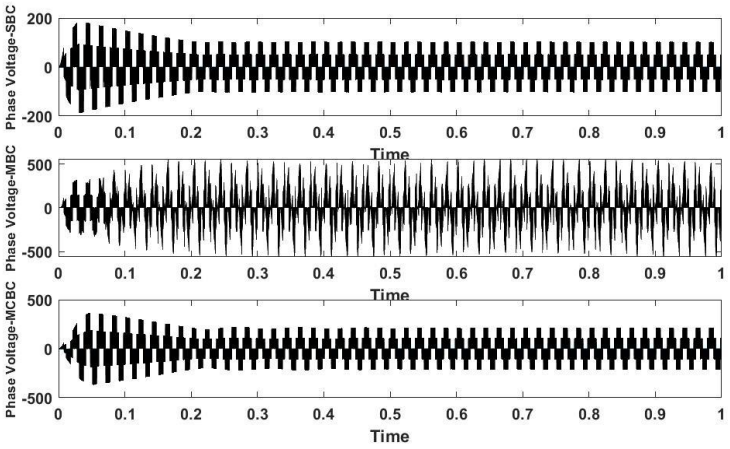

Fig. 4.8: Output Phase voltages in different control methods.

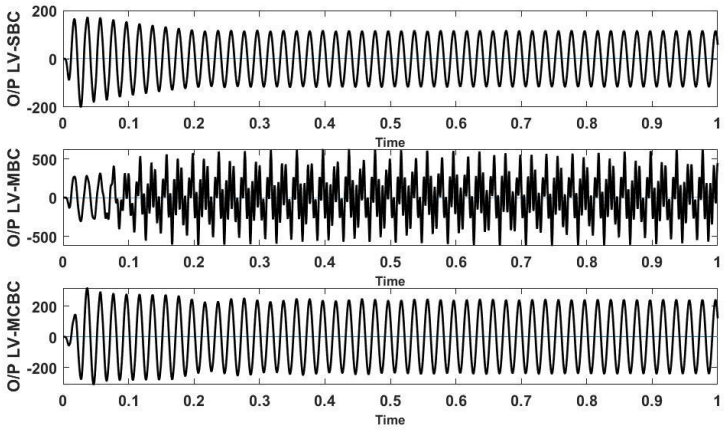

Fig. 4.9: Output Lne voltages in different control methods.

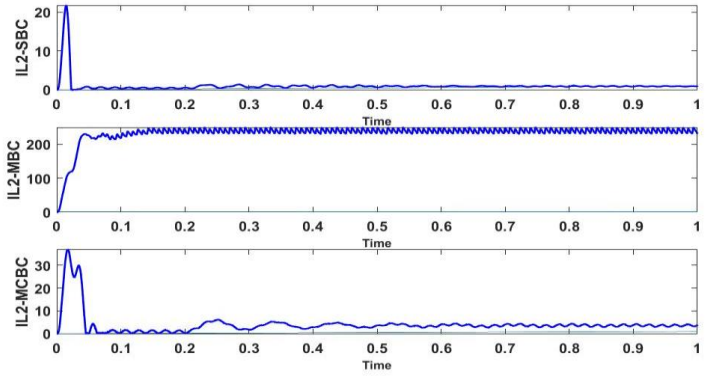

Fig. 4.10: Inductor Current (I_{L2})

Value of shoot through duty ratio (D0), Boost factor (B), Voltage across capacitors (V_{C1}, V_{C2}), DC-link, voltage across the inverter bridge (Vinv), Gain (G), RMS line voltage and Peak Value of Shoot-through Current (amp) for the modulation index 0.8 is shown in the table 3.

Table 3: Comparison of SL-QZSI for different control at .8 modulation index

Control Method	Maximum Constant Control	Maximum Boost Control	Simple Control
D_0	.307	.338	.2
B	4.48	**6.42**	2.142
V_{C1} (Volt)	114.7	152	68.57
V_{C2} (Volt)	101.6	155.25	34.28
V_{inv} (Volt)	215	308.16	102.82
Gain	3.55	**5.14**	1.71
RMS Line Voltage (Volt)	105.3	**150.96**	50.37
Peak Value of Shoot-through Current (amp)	**80**	120	35

Above simulation result are obtain for same value of modulation index, boost factor, gain and RMS Line voltage for maximum boost control is 6.42, 5.14, 150.96 V respectively

order to produce an output voltage that requires a high voltage gain, a small modulation index must be used. However, small modulation indexes result in greater voltage stress on the devices.

5. Conclusion

The maximum constant boost control of the SL-qZSI was introduced in this study, and it offers the following key benefits: continuous input current, high voltage inversion capability. Even though the voltage stress across the device only slightly rises compared to maximum boost control, this strategy is very beneficial for reducing components of the z source network (reduction of passive elements size). Furthermore, when converting a low input dc voltage to a large output ac voltage, as is the case in fuel cells or solar applications, the proposed SL-qZSI is highly helpful.

References

[1] J. S. Lai and D. J. Nelson, "Energy management power converters in hybrid electric and fuel cell vehicles," *Proc. IEEE*, vol. 95, no. 4, pp. 766–777, 2007, doi: 10.1109/JPROC.2006.890122.

[2] D. Gielen, F. Boshell, D. Saygin, M. D. Bazilian, N. Wagner, and R. Gorini, "The role of renewable energy in the global energy transformation," *Energy Strateg. Rev.*, vol. 24, pp. 38–50, Apr. 2019, doi: 10.1016/j.esr.2019.01.006.

[3] S. Adams, E. K. M. Klobodu, and A. Apio, "Renewable and non-renewable energy, regime type and economic growth," *Renew. Energy*, vol. 125, pp. 755–767, Sep. 2018, doi: 10.1016/j.renene.2018.02.135.

[4] C. Parag Jose and S. Meikandasivam, "A review on the trends and developments in hybrid electric vehicles," *Lect. Notes Mech. Eng.*, vol. PartF9, pp. 211–229, 2017, doi: 10.1007/978-981-10-1771-1_25.

[5] F. Querini, S. Dagostino, S. Morel, and P. Rousseaux, "Greenhouse gas emissions of electric vehicles associated with wind and photovoltaic electricity," in *Energy Procedia*, 2012, vol. 20, pp. 391–401. doi: 10.1016/j.egypro.2012.03.038.

[6] J. Liu, J. Wu, J. Qiu, and J. Zeng, "Switched Z-Source/Quasi-Z-Source DC-DC converters with reduced passive components for photovoltaic systems," *IEEE Access*, vol. 7, pp. 40893–40903, 2019, doi: 10.1109/ACCESS.2019.2907300.

[7] M. Meraj, S. Rahman, A. Iqbal, S. M. Ieee, L. Ben Brahim, and S. M. Ieee, "Common Mode Voltage Reduction in A Single- phase Quasi Z-Source Inverter for Transformerless Grid-Connected Solar PV Applications," *IEEE J. Emerg. Sel. Top. Power Electron.*, vol. PP, no. c, p. 1, 2018, doi: 10.1109/JESTPE.2018.2867521.

[8] F. Z. Peng, "Z-source inverter," *Conf. Rec. - IAS Annu. Meet. (IEEE Ind. Appl. Soc.*, vol. 2, pp. 775–781, 2002, doi: 10.1002/047134608x.w8348.

[9] V. Jagan and S. Das, "One switched-inductor Z-source inverter," *2017 Innov. Power Adv. Comput. Technol. i-PACT 2017*, vol. 2017-Janua, no. 8, pp. 1–6, 2017, doi: 10.1109/IPACT.2017.8244899.

[10] J. Anderson and F. Z. Peng, "Four quasi-Z-Source inverters," *PESC Rec. - IEEE Annu. Power Electron. Spec. Conf.*, pp. 2743–2749, 2008, doi: 10.1109/PESC.2008.4592360.

[11] Z. Li, G. Zhang, and C. Fang, "Enhanced switched-inductor quasi-Z-source inverter," *Beijing Hangkong Hangtian Daxue Xuebao/Journal Beijing Univ. Aeronaut. Astronaut.*, vol. 42, no. 9, pp. 1803–1811, 2016, doi: 10.13700/j.bh.1001-5965.2015.0579.

[12] M. K. Nguyen, Y. G. Jung, and Y. C. Lim, "Single-phase AC-AC converter based on quasi-Z-source topology," *IEEE Trans. Power Electron.*, vol. 25, no. 8, pp. 2200–2210, 2010, doi: 10.1109/TPEL.2010.2042618.

[13] H. Liu, Z. Zhou, Y. Li, W. Wu, J. Jiang, and E. Shi, *Impedance source inverters*. 2020. doi: 10.1007/978-981-15-2763-0.

[14] W. Liu, Y. Yang, E. Liivik, D. Vinnikov, and F. Blaabjerg, "Critical parameter analysis and design of the Quasi-Z-source inverter," *2019 IEEE 2nd Ukr. Conf. Electr. Comput. Eng. UKRCON 2019 - Proc.*, no. Dcm, pp. 474–480, 2019, doi: 10.1109/UKRCON.2019.8879831.

[15] F. Z. Peng, M. Shen, S. Member, Z. Qian, and S. Member, "Maximum Boost Control of the Z-Source Inverter," vol. 20, no. 4, pp. 833–838, 2005.

[16] P. C. Loh, D. M. Vilathgamuwa, S. Member, Y. Sen Lai, and G. T. Chua, "Pulse-Width Modulation of Z -Source Inverters," vol. 20, no. 6, pp. 1346–1355, 2005.

[17] Y. Liu, S. Member, B. Ge, H. Abu-rub, and S. Member, "Overview of Space Vector Modulations for Three- Phase Z-Source / Quasi-Z-Source Inverters," no. c.

[18] C. S. Singh and R. K. Tripathi, "Maximum Constant Boost Control of Switch Inductor Quasi Z-Source Inverter," 2013.

[19] Q. Z. P. V Inverters, A. Lashab, D. Sera, and J. M. Guerrero, "A Low-Computational High-Performance Model Predictive Control of Single Phase Battery Assisted," vol. 3.

[20] Y. Li, S. Jiang, S. Member, and J. G. Cintron-rivera, "Modeling and Control of Quasi-Z-Source In- verter for Distributed Generation Applications," no. c, 2012.

[21] A. Lashab, D. Sera, J. Martins, and J. M. Guerrero, "Model Predictive-Based Direct Battery Control in PV Fed Quasi Z-Source Inverters," no. 1, pp. 1–6.

[22] M. I. Marei, M. A. Allam, and A. Abd El-Sattar, "A simple control scheme for the high performance Z-source inverter," *Electr. Power Components Syst.*, vol. 42, no. 14, pp. 1623–1631, 2014, doi: 10.1080/15325008.2014.943440.

[23] H. Fathi and H. Madadi, "Enhanced-Boost Z-Source Inverters with Switched Z-Impedance," *IEEE Trans. Ind. Electron.*, vol. 63, no. 2, pp. 691–703, 2016, doi: 10.1109/TIE.2015.2477346.

[24] V. Jagan, J. Kotturu, and S. Das, "Enhanced-Boost Quasi-Z-Source Inverters with Two-Switched Impedance Networks," *IEEE Trans. Ind. Electron.*, vol. 64, no. 9.